

# Mechanical Vibrational Relaxation of NO on Metal and Insulator Surfaces: When and Why Are They Different?

Rongrong Yin and Bin Jiang\*

*Hefei National Laboratory for Physical Science at the Microscale, Department of Chemical Physics, Key Laboratory of Surface and Interface Chemistry and Energy Catalysis of Anhui Higher Education Institutes, University of Science and Technology of China, Hefei, Anhui 230026, China*

NO scattering from metallic and insulating surfaces represent contrasting benchmark systems for understanding energy transfer at gas-surface interface. Strikingly different behavior of highly vibrationally excited NO scattered from Au(111) and LiF(001) was observed and intuitively attributed to disparate electronic structures between metals and insulators. Here, we reveal an alternative mechanical origin of this discrepancy by comparative molecular dynamics simulations with globally accurate adiabatic neural network potentials of both systems. We find that highly-vibrating NO can reach the high dissociation barrier on Au(111), by which vibrational energy can largely transfer to translation/rotation and further dissipate into substrate phonons. This mechanical energy transfer channel is forbidden in the purely repulsive NO/LiF(001) system or for low-vibrating NO on Au(111), where molecular vibration is barely coupled to other degrees of freedom. Our results emphasize that the initial state and potential energy landscape concurrently influence the mechanical energy transfer dynamics of gas-surface scattering.

Energy exchange among molecular and surface degrees of freedom (DOFs) contributes fundamentally to various physical and chemical phenomena at gas-solid interfaces[1]. Vibrational energy transfer is of particular importance as vibrational coordinates are intrinsically relevant to forming and breaking of bonds in surface chemical reactions. This has motivated a large body of state-to-state molecular scattering experiments at solid surfaces demonstrating the most detailed dynamics on how molecular vibration couples with other DOFs[2-8]. Such state-resolved data have guided the development of theoretical models towards a predictive understanding of molecule-surface interactions[9-12].

NO scattering from solid surfaces is one of the best studied examples concerning vibrational energy transfer at gas-surface interfaces[9,13-23], due mainly to the seminal contributions of Wodtke and coworkers[24,25]. One of the most striking observations was the multi-quantum vibrational relaxation of highly vibrationally excited NO( $v_i=15$ ) scattered from Au(111)[13], compared to the large vibrational elasticity of NO( $v_i=12$ ) scattered from LiF(001)[21]. This discrepancy was intuitively attributed to the contrasting band structures of metals and insulators[13], as the mechanical (electronically adiabatic) gas-surface vibrational relaxation of small molecules was commonly recognized to be inefficient given the mismatch of molecular vibration and surface phonon frequencies[20,26]. That is to say, metals are favorable for electron transfer to NO and efficient vibration-to-electron coupling, while insulators would effectively turn off this electronically non-adiabatic vibrational relaxation channel. This concept was later supported by several different theoretical models[27-31]. In particular, the multistate-based independent electron surface hopping (IESH) model developed by Tully and

coworkers[28] qualitatively reproduced the multi-quantum vibrational relaxation of NO( $v_i=15$ ) on Au(111) at a low incidence energy ( $E_i=0.05$  eV). In comparison, adiabatic dynamics calculations on the same ground state potential energy surface (PES) resulted in large vibrational elasticity[29] as observed in previous experimental[20,21] and theoretical[26] findings for NO on LiF(001), implying similarly inefficient mechanical vibrational energy transfer in both systems.

Nevertheless, the IESH model failed to capture some more recently discovered features in the NO/Au(111) system, such as the incidence energy[18,19] and orientation[23] dependence of vibrational relaxation and the final translational energy distributions[19]. These failures were attributed to the inaccuracy of the empirical function parameterized adiabatic PES used in IESH simulations[18], which have been largely remedied by a more accurate machine learned adiabatic NO/Au(111) PES developed by us based on thousands of density functional theory (DFT) data points[32]. Combining this PES with the orbital-dependent electronic friction tensor accounting for non-adiabatic effects[33], diverse experimental observations have been reasonably reproduced. This new PES predicted a surprisingly large amount of vibrational energy of the highly-vibrating NO dissipated mechanically into the gold surface[32], suggesting that the efficiency of mechanical gas-surface vibrational relaxation is not always low and is very dependent on the adiabatic PES. In this Letter, we develop a new high-quality machine learned PES for NO scattering from LiF(001) fit to numerous DFT data. With the state-of-the-art adiabatic PESs for both systems, we are able to elucidate how the observed distinct vibrational inelasticity of NO scattered from metals and insulators is related to their

adiabatic PESs and in which condition the molecular vibrational energy is able to flow into substrate phonons despite the mismatch of their frequencies.

To construct the PES, periodic DFT calculations were performed using the Vienna ab Initio Simulation Package (VASP)[34,35] with the PW91 functional[36]. The LiF(001) surface was modeled with a four-layer slab in a  $2 \times 2$  supercell, in which the top two layers were movable. The plane-wave basis set was truncated at 400 eV and Brillouin-zone was sampled by a  $5 \times 5 \times 1$  Monkhorst-Pack  $k$ -points mesh. To map out the PES including both molecular and surface DOFs, we collected 3608 data points using an adaptive sampling strategy[37] that fully cover the configuration space relevant to highly vibrationally excited NO scattering from LiF(001). Both energies and forces were trained using our recently proposed embedded atom neural network (EANN) approach[38-40]. The NO/Au(111) PES used here was also retrained with EANN using the DFT data in Ref. [32]. To calculate the state-to-state scattering probabilities of NO and account for the large energy exchange between the heavy molecule and the substrate, which is intractable at present by a fully-coupled quantum dynamics method, we carried out quasi-classical trajectory (QCT) calculations with the initial and final conditions of NO molecules quantized semiclassically. Such a treatment has shown to be reliable for diatomic scattering from surfaces, *e.g.* for molecular hydrogen[10]. More details about the EANN PES and QCT simulations are given in the Supplemental Material (SM).

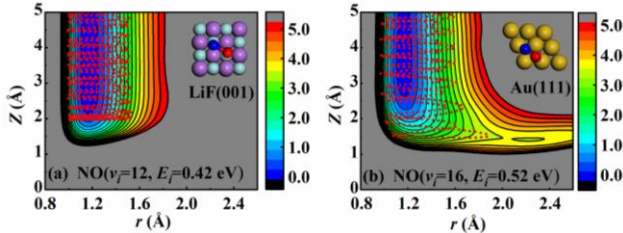


FIG. 1. Two-dimensional cuts of (a) the NO/LiF(001) and (b) the NO/Au(111) PESs as a function of the N-O distance ( $r$ ) and the molecular height ( $Z$ ) above the surface, in which the molecular orientations are both kept as that at the transition state on Au(111), and the molecular center is fixed on the hollow site on LiF(001) and bridge site on Au(111), respectively, and surface atoms are all fixed at equilibrium. A representative trajectory (red dots) of each system is projected on top of the corresponding PES.

Let us first look at the first-principles-determined potential energy landscapes of the NO/Au(111) and NO/LiF(001) systems. As displayed in Fig. 1, the biggest difference between the two PESs is that NO is dissociative on Au(111) with a high barrier of  $\sim 2.86$  eV with its bond length elongated to  $\sim 1.89$  Å, while is absolutely non-dissociative and repulsive on LiF(001). Additionally, the NO molecular adsorption energy is higher on Au(111) than on LiF(001) (0.39 eV *versus* 0.06 eV). Accordingly, the NO/Au(111) PES is much more anisotropic and corrugated than the NO/LiF(001) PES, as displayed in Fig. S3-5. These

differences clearly reflect a stronger interaction of NO with a metal than with an ionic crystal.

Keeping this in mind, we discuss the adiabatic energy transfer dynamics in these two systems in similar conditions. Fig. 2 compares the calculated final vibrational state ( $v_f$ ) distributions of highly vibrationally excited NO molecules scattered from both surfaces, with available experimental data[13,41] at surface temperature ( $T_s$ ) of  $\sim 300$  K. Although electronically non-adiabatic effects are not included, we see an obvious difference in the two cases. NO( $v_i=16$ ,  $E_i=0.52$  eV) scattering from Au(111) undergoes multi-quantum vibrational relaxation yielding a broad vibrational state distribution down to  $v_f \approx 2$  and peaking at  $v_f \approx 10$ . This amounts roughly to half of the experimentally measured vibrational relaxation[19]. Our recent work showed that the agreement with experiment in this and other conditions can be further largely improved if hot-electron effects were taken into account by the electronic friction theory with the orbital-dependent friction tensor and reasonable corrections to the Markovian approximation[33]. On the contrary, our calculations predict absolute vibrational elasticity of NO( $v_i=12$ ,  $E_i=0.42$  eV) scattered from LiF(001), in good accord with the high survival probability observed in experiment. Apparently, the much more significant vibrational relaxation of highly vibrationally excited NO from Au(111) than from LiF(001) cannot be explained by the direct vibration-phonon coupling. Fig. S6 shows that phonon frequencies of LiF(001) are generally several times higher than those of Au(111), relatively closer to the NO vibrational frequency ( $1906 \text{ cm}^{-1}$ ). This should enable faster vibrational relaxation rate of NO on LiF(001) in terms of the energy gap law for vibrational energy transfer[26].

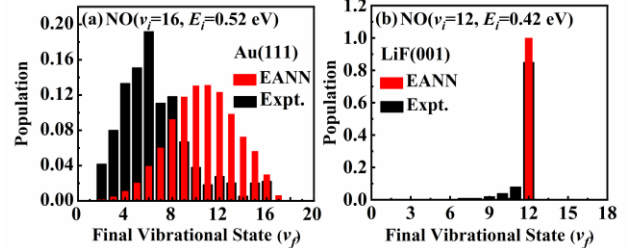


FIG. 2. Comparison of vibrational state distributions of highly vibrationally excited NO scattered from (a) Au(111) and from (b) LiF(001), including the adiabatic QCT results on the EANN PES (red) and experimental data (black). Initial conditions are selected mimicking the corresponding experiments.

Different adiabatic energy transfer dynamics in the two cases can be further seen in the energy partitioning of scattered molecules. Table I compares the mean values of the rotational ( $\langle \Delta E_{rot} \rangle$ ), vibrational ( $\langle \Delta E_{vib} \rangle$ ), translational ( $\langle \Delta E_{trans} \rangle$ ) and total energy loss ( $\langle \Delta E_{tot} \rangle$ ) of NO scattering from LiF(001) and Au(111), defined by the final energy minus the initial energy of NO. Although there is negligible vibrational energy loss of NO( $v_i=12$ ) on LiF(001), about half of the translational energy is lost to the lattice, along with slight rotational excitation. This indicates that molecular

vibration is barely coupled to other molecular and surface DOFs, originating from the purely repulsive, nearly isotropic and flat PES in this system (see Fig. 1 and S3-5). To illustrate this more explicitly, a representative trajectory of NO( $v_i=12$ ,  $E_i=0.42$  eV) scattering from LiF(001) is projected onto Fig. 1a, where the vibrational motion is completely orthogonal to translation, whose amplitude is basically unperturbed upon the direct scattering process. Fig. 3a further shows that the mechanical energy exchange between molecular translation and the LiF lattice occurs upon a short contact with the surface. The NO molecule quickly converts all of its translational energy to potential energy at the repulsive wall, then gets only half of kinetic energy back when recoiling from the surface, resulting in a net translational energy loss to surface phonons. Interestingly, this vibrational elasticity and translational inelasticity of NO scattering from LiF(001) is insensitive to the incidence energy, initial vibrational state, and surface temperature, as in any cases NO would undergo more or less the same repulsive force with negligible vibration-to-translation (V-T) coupling. Indeed, we find again no vibrational de-excitation of NO( $v_i=1$ ) scattered from LiF(001) at  $E_i=0.31$  eV, in line with the large survival probability in experiment ( $\sim 0.9 \pm 0.1$ ) in the same condition[20]. The average final translational energy of scattered molecules is  $\sim 0.21$  eV, which compares well with the experimental value ( $\sim 0.19$  eV)[20]. The measured narrow angular distribution and low rotational temperature[20] are also well reproduced. These results suggest that the scattering dynamics of NO from LiF(001) is well described by the new PES (see SM for additional results).

Table I. Average rotational, vibrational, translational, and total energy losses (in eV) of NO before and after scattering from LiF(001) and Au(111) in various initial conditions (see text).

Mean energy loss (eV)	LiF(001)		Au(111)	
	NO( $v_i=12$ ) $E_i=0.42$ eV	NO( $v_i=1$ ) $E_i=0.31$ eV	NO( $v_i=16$ ) $E_i=0.52$ eV	NO( $v_i=1$ ) $E_i=0.31$ eV
$\langle \Delta E_{rot} \rangle$	0.035	0.037	0.40	0.055
$\langle \Delta E_{vib} \rangle$	-0.0010	-0.0013	-1.0	-0.0020
$\langle \Delta E_{trans} \rangle$	-0.24	-0.10	-0.036	-0.13
$\langle \Delta E_{tot} \rangle$	-0.20	-0.063	-0.65	-0.077

In sharp contrast, NO( $v_i=16$ ,  $E_i=0.52$  eV) scattered from Au(111) loses a substantial amount of vibrational energy ( $\langle \Delta E_{vib} \rangle = -1.0$  eV) and only a little translational energy ( $\langle \Delta E_{trans} \rangle = -0.036$  eV), flowing primarily into the lattice ( $\langle \Delta E_{tot} \rangle = -0.65$  eV) and partly to rotation ( $\langle \Delta E_{rot} \rangle = 0.40$  eV). Unlike the NO/LiF(001) case, now the highly-vibrating NO molecule has an opportunity to lengthen and dissociate on Au(111)[32], during which the molecular vibration can gradually soften and thus couple with other DOFs. Fig. S7 demonstrates the mode softening from  $1906 \text{ cm}^{-1}$  in the gas phase to  $457 \text{ cm}^{-1}$  at the transition state along the minim energy path. Similar mode softening has effectively lowered the vibrationally adiabatic barrier height and enabled great

vibrational enhancement of dissociative adsorption of polyatomic molecules at metal surfaces[42]. Its influence on vibrationally inelastic scattering is clearly seen via a representative trajectory of NO( $v_i=16 \rightarrow v_f=10$ ) scattering from Au(111) in Fig. 1b and the corresponding kinetic energy evolution in each DOF as a function of time in Fig. 3d-e. In this case, before the first impact at the surface ( $Z > 2.0$  Å), the NO molecule has acquired additional translational energy by  $\sim 0.89$  eV with its bond length slightly extended to  $\sim 1.65$  Å. Note that the NO-Au(111) attraction may accelerate the NO molecule by at most  $\sim 0.39$  eV (*i.e.*, the maximum adsorption well depth), but the excess translational energy gain must be transferred from vibration as a result of V-T coupling. As the molecule goes more deeply to the repulsive wall and elongates further to the transition state region, the vibration is more significantly softened and the translation is suppressed. Both the vibrational kinetic energy and translational energy largely decrease, accompanied with a rapid increase of the kinetic energy of surface atoms (of course also the potential energy of the system, which is however inseparable). Meanwhile, a large amount of energy is transferred to molecular rotation because the PES in this region features strong anisotropy and corrugation (Figs. S3-5) and the molecule would reorient to resemble the transition state geometry. Whereas the bond dissociation is unsuccessful and the molecule is eventually scattered back to the vacuum leaving the highly excited surface phonons and molecular rotation, yet much reduced vibrational excitation. Interestingly, even running calculations with all surface atoms fixed, we still see significant vibrational energy loss ( $\langle \Delta E_{vib} \rangle = -0.71$  eV) of NO scattered from Au(111) but with a net average energy gain in translation ( $\langle \Delta E_{trans} \rangle = 0.22$  eV) and rotation ( $\langle \Delta E_{rot} \rangle = 0.49$  eV). This signifies that a large fraction of translational energy and part of rotational energy transferred from vibration eventually flows to surface phonons in the strongly interacting region when the surface is relaxed.

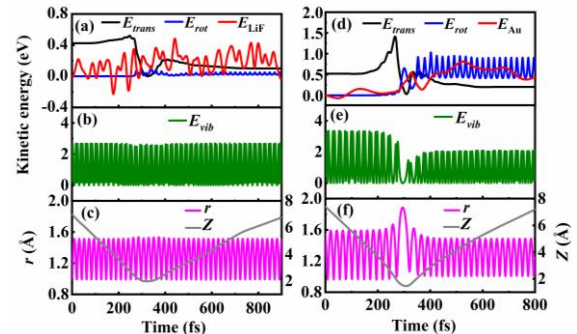


FIG. 3. Kinetic energy and geometric evolutions as a function of time during a representative scattering trajectory for NO( $v_i=12$ ,  $E_i=0.42$  eV) from LiF(001) (a-c) and NO( $v_i=16$ ,  $E_i=0.52$  eV) from Au(111) (d-f), including the kinetic energy in NO translation ( $E_{trans}$ , black), rotation ( $E_{rot}$ , blue), and vibration ( $E_{vib}$ , green), the average kinetic energy of surface atoms relative to the initial value ( $E_{LiF}$  and  $E_{Au}$ , red), the N-O distance ( $r$ , magenta), and the molecular height ( $Z$ , gray).

We emphasize that such efficient adiabatic vibrational energy transfer would happen for highly vibrationally excited states of NO on Au(111) only. Indeed, the scattering of NO( $v_i=1$ ,  $E_i=0.31$  eV) from Au(111) turns out to be more similar to that from LiF(001), giving rise to nearly no vibrational energy loss (see Table I). Moreover, the mean translational energy loss of NO is 0.13 eV on Au(111), comparable to that on LiF(001). As illustrated in Fig. S8, this is because that NO( $v_i=1$ ) cannot feel the barrier for dissociation on Au(111) and directly scatters in the entrance channel, having a similar behavior as on the repulsive LiF(001) surface. We have found that mechanical vibrational de-excitation becomes measurable for NO( $v_i=3$ ) and increasingly significant as  $E_i$  increase[32], as the molecule is more strongly affected by the force of the transition state region. The influence of the dissociation barrier on gas-surface scattering has been mainly discussed in systems with relatively low barriers and for low vibrational states[4,7,43,44]. Our results highlight that the scattering of highly vibrationally excited molecules at solid surfaces can be strongly affected by the very high barrier that is customarily ignored. This explains the negligible vibrational relaxation in adiabatic dynamics calculations on the empirical PES without a dissociation barrier[29].

With this more quantitative understanding of vibrational relaxation at gas-surface interfaces, we turn to discuss the remaining discrepancy between theory and experiment for NO( $v_i=12$ ) scattering from LiF(001). Defects in experimentally prepared LiF(001) samples have been invoked to explain the observed minor vibrational inelasticity of NO( $v_i=12$ )[41]. The influence of defects can be remarkable, for example, NO( $v_i=1$ ) scattering was found completely vibrationally inelastic[45] from polished LiF(001) (with possibly high concentration of defects), while mostly vibrationally elastic[20] from well-cleaved LiF(001). By performing additional DFT calculations on defective LiF(001) surfaces with steps or ionic vacancies (see the SM for details), we find that those defects only moderately strengthen the NO-LiF binding but fail to support any dissociation transition states. Based on our analysis, however, the mechanical vibrational relaxation would be significant only if the repulsive PES was largely changed to enable some sort of dissociation. On the other hand, we find that a single Li<sup>+</sup> vacancy can significantly reduce the band gap of LiF(001) to  $\sim 2.40$  eV, which may fall in the energy range accessible by NO( $v_i=12$ ) with a vibrational energy of  $\sim 2.70$  eV and enable the vibration-to-electron coupling. These findings suggest that defects may cause some non-adiabatic vibrational energy loss of NO on imperfect LiF(001). Additional work is needed to confirm this.

To summarize, we report a comparative study on the adiabatic energy transfer dynamics of NO scattering from Au(111) and LiF(001), using two high-dimensional global neural network PESs with DFT accuracy. We find almost exclusive vibrationally elastic products of NO( $v_i=12$ ) scattered from LiF(001), in stark contrast with the multi-

quantum relaxation NO( $v_i=16$ ) from Au(111). However, the scattering of NO( $v_i=1$ ) from both surfaces is vibrationally elastic and only translational energy leads to phonon excitation. This interesting discrepancy and similarity have been quantitatively rationalized by the potential energy landscape accessible by the impinging NO molecule. As long as the molecule reaches the dissociation barrier region, its vibration will be significantly softened and vibration-to-translation/rotation/phonon energy transfers are significant. While the low-vibrating NO molecule is rejected directly by the repulsive wall without experiencing the dissociative force and the vibrational softening on Au(111), rendering its similar behavior as on the purely repulsive LiF(001) surface. Our results not only reproduce well the experimental data for NO scattering on LiF(001), but also suggest a mechanical mechanism for the discrepant vibrational relaxation of highly-vibrating NO scattering at metallic and insulating surfaces. An apparent next step is to combine this mechanical and the electron-mediated non-adiabatic vibrational energy transfer channels, which could be both promoted by the same region of the PES[22], to fully understand the energy transfer dynamics of molecules like NO and CO at metal surfaces.

We appreciate the support from National Key R&D Program of China (2017YFA0303500), National Natural Science Foundation of China (21722306, 22073089), Anhui Initiative in Quantum Information Technologies (AHY090200). We thank Prof. Alec Wodtke for some helpful discussion.

---

\*bjiangch@ustc.edu.cn

- [1] G. B. Park, B. C. Krüger, D. Borodin, T. N. Kitsopoulos, and A. M. Wodtke, Reports on Progress in Physics **82**, 096401 (2019).
- [2] C. T. Rettner, F. Fabre, J. Kimman, and D. J. Auerbach, Phys. Rev. Lett. **55**, 1904 (1985).
- [3] B. D. Kay, T. D. Raymond, and M. E. Coltrin, Phys. Rev. Lett. **59**, 2792 (1987).
- [4] C. T. Rettner, D. J. Auerbach, and H. A. Michelsen, Phys. Rev. Lett. **68**, 2547 (1992).
- [5] Q. Ran, D. Matsiev, D. J. Auerbach, and A. M. Wodtke, Phys. Rev. Lett. **98**, 237601 (2007).
- [6] K. Golibrzuch, P. R. Shirhatti, J. Altschaffel, I. Rahinov, D. J. Auerbach, A. M. Wodtke, and C. Bartels, J. Phys. Chem. A **117**, 8750 (2013).
- [7] J. Geweke, P. R. Shirhatti, I. Rahinov, C. Bartels, and A. M. Wodtke, J. Chem. Phys. **145**, 054709 (2016).
- [8] J. Werdecker, M. E. van Reijzen, B.-J. Chen, and R. D. Beck, Phys. Rev. Lett. **120**, 053402 (2018).
- [9] K. Golibrzuch, N. Bartels, D. J. Auerbach, and A. M. Wodtke, Annu Rev Phys Chem **66**, 399 (2015).
- [10] G.-J. Kroes and C. Diaz, Chem. Soc. Rev. **45**, 3658 (2016).

- [11] M. Alducin, R. D éz Mui ño, and J. I. Juaristi, *Prog. Surf. Sci.* **92**, 317 (2017).
- [12] B. Jiang and H. Guo, *J. Chem. Phys.* **150**, 180901 (2019).
- [13] Y. Huang, C. T. Rettner, D. J. Auerbach, and A. M. Wodtke, *Science* **290**, 111 (2000).
- [14] Y. Huang, A. M. Wodtke, H. Hou, C. T. Rettner, and D. J. Auerbach, *Phys. Rev. Lett.* **84**, 2985 (2000).
- [15] R. Cooper *et al.*, *Angew Chem Int Ed Engl* **51**, 4954 (2012).
- [16] K. Golibrzuch, P. R. Shirhatti, J. Altschaffel, I. Rahinov, D. J. Auerbach, A. M. Wodtke, and C. Bartels, *J Phys Chem A* **117**, 8750 (2013).
- [17] N. Bartels, B. C. Kruger, D. J. Auerbach, A. M. Wodtke, and T. Schafer, *Angew. Chem. Int. Ed.* **53**, 13690 (2014).
- [18] K. Golibrzuch, P. R. Shirhatti, I. Rahinov, A. Kandratsenka, D. J. Auerbach, A. M. Wodtke, and C. Bartels, *J. Chem. Phys.* **140**, 044701 (2014).
- [19] B. C. Kruger, N. Bartels, C. Bartels, A. Kandratsenka, J. C. Tully, A. M. Wodtke, and T. Schafer, *J. Phys. Chem. C* **119**, 3268 (2015).
- [20] J. Misewich, H. Zacharias, and M. M. T. Loy, *Phys. Rev. Lett.* **55**, 1919 (1985).
- [21] A. M. Wodtke, Y. Huang, and D. J. Auerbach, *The Journal of Chemical Physics* **118**, 8033 (2003).
- [22] B. C. Krüger, S. Meyer, A. Kandratsenka, A. M. Wodtke, and T. Schäfer, *The Journal of Physical Chemistry Letters* **7**, 441 (2016).
- [23] N. Bartels, K. Golibrzuch, C. Bartels, L. Chen, D. J. Auerbach, A. M. Wodtke, and T. Schafer, *J. Chem. Phys.* **140**, 054710 (2014).
- [24] A. M. Wodtke, D. Matsiev, and D. J. Auerbach, *Prog. Surf. Sci.* **83**, 167 (2008).
- [25] A. M. Wodtke, *Chem Soc Rev* **45**, 3641 (2016).
- [26] R. R. Lucchese and J. C. Tully, *J. Chem. Phys.* **80**, 3451 (1984).
- [27] S. Li and H. Guo, *J. Chem. Phys.* **117**, 4499 (2002).
- [28] N. Shenvi, S. Roy, and J. C. Tully, *J. Chem. Phys.* **130**, 174107 (2009).
- [29] N. Shenvi, S. Roy, and J. C. Tully, *Science* **326**, 829 (2009).
- [30] S. Monturet and P. Saalfrank, *Physical Review B* **82**, 075404 (2010).
- [31] S. Roy, N. A. Shenvi, and J. C. Tully, *J. Chem. Phys.* **130**, 174716 (2009).
- [32] R. Yin, Y. Zhang, and B. Jiang, *The Journal of Physical Chemistry Letters* **10**, 5969 (2019).
- [33] C. L. Box, Y. Zhang, R. Yin, B. Jiang, and R. J. Maurer, 2020), p. arXiv:2010.05325.
- [34] G. Kresse and J. Furthmuller, *Phys. Rev. B* **54**, 11169 (1996).
- [35] G. Kresse and J. Furthmuller, *Comp. Mater. Sci.* **6**, 15 (1996).
- [36] J. P. Perdew, J. A. Chevary, S. H. Vosko, K. A. Jackson, M. R. Pederson, D. J. Singh, and C. Fiolhais, *Phys. Rev. B* **46**, 6671 (1992).
- [37] Y. Zhang, X. Zhou, and B. Jiang, *J. Phys. Chem. Lett.* **10**, 1185 (2019).
- [38] Y. Zhang, C. Hu, and B. Jiang, *J. Phys. Chem. Lett.* **10**, 4962 (2019).
- [39] L. Zhu, Y. Zhang, L. Zhang, X. Zhou, and B. Jiang, *Phys. Chem. Chem. Phys.* **22**, 13958 (2020).
- [40] Y. Zhang, R. J. Maurer, and B. Jiang, *J. Phys. Chem. C* **124**, 186 (2020).
- [41] A. M. Wodtke, Y. Huang, and D. J. Auerbach, *J. Chem. Phys.* **118**, 8033 (2003).
- [42] S. Nave, A. K. Tiwari, and B. Jackson, *J. Phys. Chem. A* **118**, 9615 (2014).
- [43] M. del Cueto, X. Zhou, A. S. Muzas, C. D áz, F. Mart ín, B. Jiang, and H. Guo, *J. Phys. Chem. C* **123**, 16223 (2019).
- [44] J. Werdecker, B.-J. Chen, M. E. Van Reijzen, A. Farjammia, B. Jackson, and R. D. Beck, *Physical Review Research* **2**, 043251 (2020).
- [45] H. Zacharias, M. M. T. Loy, and P. A. Roland, *Phys. Rev. Lett.* **49**, 1790 (1982).